Research in Pharmaceutical Sciences, August 2021; 16(4): 370-380
Received: 23-09-2020
Peer Reviewed: 28-10-2020
Revised: 30-11-2020
Accepted: 22-04-2021
Published: 30-06-2021

School of Pharmacy & Pharmaceutical Sciences
Isfahan University of Medical Sciences

Original Article

Hepatoprotective effect of kaempferol glycosides isolated from *Cedrela odorata L.* leaves in albino mice: involvement of Raf/MAPK pathway

Gihan Farag Asaad[1,*], Heba Mohammed Ibrahim Abdallah[1], Hala Shaaban Mohammed[2], and Yousra Ahmed Nomier[3]

[1]National Research Centre, Pharmacology Department, Medical Research Divison, Giza, Egypt.
[2]Pharmacognosy Department, Faculty of Pharmacy-Al-Azhar University, Cairo, Egypt.
[3]Pharmacology and Toxicology Department, Pharmacy College, Jazan University, Saudi Arabia.

Abstract

Background and purpose: Paracetamol is the most implicated xenobiotic in inducing hepatotoxicity. Our study aimed to determine the impact of some kaempferol glycosides isolated from the leaves of *Cedrela odorata* L. on paracetamol hepatotoxicity.

Experimental approach: The methanolic extract of dried leaves of *C. odorata L.* was subjected to the combination of spectroscopic methods (^{1}H and ^{13}CNMR). Six kaempferol glycosides were isolated: kaempferol-3-*O*-β-D-glycopyranoside (astragalin), kaempferol-3-*O*-β-L-rhamnopyranoside, kaempferol-3-*O*-β-D-rutinoside, kaempferide-3-*O*-β-D-rutinoside, kaempferide-3-*O*-β-Drutinosyl-7-*O*-β-D-rhamnopyranoside, and kaempferol-3-*O*-β-D- rutinosyl-7-*O*-α-D-arabinopyranoside. Fifty-four female Swiss Albino mice were divided randomly into 9 groups including (1) control negative (1 mL/kg saline; IP), (2) control positive (paracetamol 300 mg/kg; IP), (3) silymarin 50 mg/kg (IP). Animals of groups 4-9 were injected with 6 different samples of isolated compounds at 100 mg/kg (IP). One h later, groups 3-9 were injected with paracetamol (300 mg/kg IP). Two h later, tissue samples were taken from all animals to assess nitrotyrosine, c-Jun N-terminal protein kinase (c-JNK), Raf -1kinase, and oxidative stress biomarkers *viz.* reduced glutathione (GSH) and malondialdehyde (MDA).

Findings/Results: Isolated glycosides had a prominent anti-apoptotic effect *via* inhibition of c-JNK and Raf-1 kinase. They also exerted a powerful antioxidant effect by modulating the oxidative stress induced by paracetamol *via* increasing GSH, reducing MDA and nitrotyrosine concentrations compared to positive control. The glycoside (1) showed a better effect than silymarin (standard) in ameliorating the formation of nitrotyrosine, Raf-1 kinase, c-JNK, and GSH.

Conclusion and implication: Kaempferol glycosides isolated for the first time from *C. odorata* L. leaves exerted antioxidant and antiapoptotic effects *via* amelioration of oxidative stress and inhibition of Raf/ MAPK pathway.

Keywords: Antioxidant; *C. odorata L;* Glycosides; Kaempferol; Nitrotyrosine; Paracetamol; Raf/MAPK.

INTRODUCTION

Paracetamol (acetaminophen) is a strong analgesic and antipyretic. However, it exerts hepatotoxicity when unintentionally ingested once at high doses or even when given at therapeutic doses for a prolonged time (1). Paracetamol is now the principal cause of acute liver failure in many Western countries (2). The paracetamol-induced hepatotoxicity is evidenced by the production of its metabolite, N-acetyl-p-benzoquinone imine (NAPQI) that can be successfully scavenged by reduced glutathione (3)

Access this article online

Website: http://rps.mui.ac.ir

DOI: 10.4103/1735-5362.319575

*Corresponding author: G.F. Asaad
Tel: +20-1011277968; Fax: +20-23370931
Email: dr_g.asaad@yahoo.com

It is now believed that mitochondrial damage is central to the toxicity of paracetamol. Treatment with paracetamol is attributed to various mitochondrial alterations, *viz* morphological abnormalities, reduced respiration, and oxidative stress (4-6). The initial reactive oxygen species (ROS) formation leads to activation of Raf-1 protein kinase which in turn activates the mitogen-activated protein kinase (MAPK) and c-Jun N-terminal kinase (JNK) (7). Modulation of Raf/MAPK signaling pathway in response to paracetamol toxicity contributes to uncontrollable cell apoptosis evidenced by activation of these kinases (8).

Nowadays, many studies are targeting the discovery of natural products either to replace the synthetic medicinal agents for avoiding their adverse effects or in order to increase the use of current chemical agents *via* reducing their detrimental effects. *Cedrela odorata L.* is the most commercially important and widely distributed species in the genus *Cedrela*. It is well known in traditional medicine and used as a house remedy by the decoction of its leaves. The bark is used to treat wounds, fever, bronchitis, indigestion, and other gastrointestinal ailments (9). Polyphenolic extract of *C. odorata L.* barks was found to reduce hepatic lipid peroxidation in diabetic rats. It also reduced cholesterol levels in a hypercholesterolemic mouse model and decreased hepatic lipid peroxidation (10). In another study, the hydroethanolic extract of the inner stem park of *C. odorata L.* blunted the postprandial hyperglycemia in rats due to inhibition of α- glucosidase and enhancement of the antioxidant enzymes (11) but the bioactive components leading to these effects were not identified.

Hence, the current study aimed to identify the ingredients isolated from the dried methanolic extract of *C. odorata* L. leaves and then to investigate their hepatoprotective activity against paracetamol-induced hepatotoxicity in mice. The antioxidant and antiapoptotic effects of these flavonoids have been studied as potential underlying mechanisms by assessment of reduced glutathione (GSH), malondialdehyde (MDA), nitrotyrosine, Raf-1 protein kinase, and c-JNK.

MATERIAL AND METHODS

Plant material

The leaves of *C. odorata* L. were collected from zoological garden in Giza-Egypt in September 2015 and identified by Dr. Mohammed El-Gebaly, Department of Botany, National Research Centre (NRC) and by Mrs. Tereez Labib Consultant of Plant Taxonomy at the Ministry of Agriculture and director of Orman botanical garden, Giza, Egypt. A voucher specimen (Reg. No. 2015 C.o. 81) is deposited in the herbarium of Pharmacognosy Department, Faculty of Pharmacy, Al Azhar University, Cairo, Egypt.

Chemical agents

Proton and carbon-13 nuclear magnetic resonance (^{1}HNMR and ^{13}CNMR) (king Abdul-Aziz University, Gedda, Saudi Arabia, BRUKER 850 MHz for ^{1}H and 213 MHz for ^{13}C (Bruker, China), Cairo University-Faculty of Pharmacy BRUKER400 for ^{1}H MHz and 100 MHz for ^{13}C) (Bruker, China), polyamide 6S for column chromatography, sephadex LH-20, silica gel for column chromatography, and 2D-paper chromatography (Sigma-Aldrich, Egypt). Thin-layer chromatography (TLC) F254 plates (Sigma-Aldrich, Egypt). Mobile phases; butanol:acetic acid:water (4:1:5 v/v upper phase), aqueous acetic acid (15% and 85:15 v/v, methylene chloride, butanol, ethyl acetate). Spraying reagents ($AlCl_3$, $FeCl_3$, ethanol/sulphuric, NH_4OH and aniline hydrogen sulfate). Paracetamol and silymarin were purchased from (Sigma Chemical Company, St. Louis, MO, USA).

Animals

Fifty-four female Swiss Albino mice weighing 20-30 g were purchased from National Research Centre breeding unit and were divided randomly into 9 groups, 6 each. This study was approved by the ethical committee of the National Research Centre with approval ethical number: 17-130. The study was also conducted according to the National Regulations on Animal Welfare and Institutional Animal Ethical Committee (IAEC).

Preparation of plant extract

The dry ground leaves of *C. odorata* L. (700 g) were extracted with 70% methanol/water under reflux (7 × 3L) then, the aqueous methanol was evaporated under reduced pressure. The totally dried extract was subjected to the defatting process with methylene chloride under reflux. Then the residue after defatting was precipitated by water:ethanol (1:10) to precipitate inorganic salts and sugars. After precipitation, the filtrate was evaporated under reduced pressure. Many fractions were obtained from polyamide column, then the similar fraction was collected to obtain five fractions. Then collective fractions (2-5), respectively were purified by means of sephadex LH-20 column chromatography using different mobile phases: ethanol (100%) and butanol:isopropyl:water (4:1:5 v/v upper phase) to obtain six compounds; 1-6.

Experimental protocol

All animals were fasted 12 h before performing the experiment. Mice were randomly divided into 9 groups, 6 each. Group 1 was kept as control negative (1 mL/kg physiological saline; IP) and group 2 was the control positive (injected with paracetamol 300 mg/kg; IP) (12). Animals of group 3 were injected with silymarin as a standard drug (50 mg/kg; IP). Animals of group 4-9 were injected with the 6 isolated compounds from *C. odorata L*. leaves (100 mg/kg; IP). One h after an injection of all isolated compounds and standard drug, all groups except the control negative were injected with paracetamol (300 mg/kg; IP). Two h later, animals were sacrificed by cervical dislocation under anesthesia of pentobarbital sodium. Liver samples were kept frozen at -80 °C for the quantitative determination of GSH, MDA, nitrotyrosine adducts, Raf-1 kinase, and c-Jun N-terminal protein kinase.

Biochemical analysis

Oxidative stress biomarkers in liver tissue

GSH assessment is based on the reduction of 5,5-dithiobis-2-nitrobenzoic acid to produce a yellow compound. The reduced chromogen is directly proportional to GSH concentration and its absorbance can be measured spectrophotometrically at 405 nm using a commercial kit (Biodiagnostic, Egypt) (13); MDA, a reactive aldehyde that is an indicator of lipid peroxidation, was determined using a spectrophotometer. The absorbance of the MDA forms colored complexes was measured spectrophotometrically at 532 nm (14). All samples were calculated per mg total protein in each sample.

Nitrotyrosine adducts

Nitrotyrosine formation is a footprint of peroxynitrite production. The hepatic nitrotyrosine levels were assayed using the quantitative sandwich enzyme immunoassay method (Rat 3-nitrotyrosine ELISA Kit, catalog No. MBS732683, MyBiosource. Inc, San Deigo, USA). The procedure was done according to the manufacturer's instructions. The optical density was adjusted at 450 nm.

Apoptotic biomarkers

Raf-1 protein kinase

This ELISA kit is a 1.5-h solid-phase ELISA designed for the quantitative determination of rat phospho Raf-1. Phospho Raf-1 (ser301) ELISA kit (catalog No. MBS7218211, MyBiosource. Inc, San Deigo, USA) applies the competitive enzyme immunoassay technique utilizing a monoclonal anti-antibody and HRP conjugate. The optical density was adjusted at 450 nm.

C-Jun N-terminal protein kinase

An immune assay for the quantitative determination of JNK 1/2 dual phosphorylated at threonine 183 and tyrosine 185 in cell lysates using ELISA kit (JNK 1/2 [pT183/pY185] ELISA kit, catalog No. KHO0511, Invitrogen Corporation. CA, USA). The concentration of C-Jun N-terminal protein kinase was determined by ELISA and the optical density was adjusted at 450 nm.

Statistical analysis

Data were presented as mean ± SEM. Statistical analysis was carried out by one-way analysis of variance (ANOVA) followed by Tukey's test for multiple comparisons. $P < 0.05$ was considered significant.

RESULTS

Phytochemistry identification

The isolated phytoconstituents from the leaves of *C. odorata* L. were brilliant yellow amorphous powder, it was observed as dark purple fluorescence under long and short UV-light; which turned to dull yellow florescence with ammonia vapor under UV-light.

Compound (1), an A_2-X_2 spin coupling system of two ortho-doublets, each of two protons, were assigned at 7.98 and 6.88 with J-value of 8.5 Hz for H2$^{/}$/6$^{/}$and H3$^{/}$/5$^{/}$of 1, 4-disubstituted of B-ring. Also, meta-doublets, each of one proton, were established for H-8 and H-6 at 6.42 and 6.21 (d, J = 1.8 Hz and 2.0 Hz) respectively, for 5, 7-dihydroxy A-ring. In the aliphatic region, the anomeric proton signal was assigned at 5.31 (d, J = 7.5 Hz) to confirm a β-pyranoside structure of glucoside moiety.^{13}CNMR showed 13 carbon resonances characteristic of kaempferol aglycone among which five signals at 177.38 (C-4) and 133.21 (C-3) of C-ring, 159.89 (hydroxylated C-4$^{/}$), 130.88 (C2$^{/}$/6$^{/}$) and 115.09 (C3$^{/}$/5$^{/}$) of B-ring. Analysis of ^{1}HNMR and ^{13}CNMR spectra of compound (1) and comparison of the previous values reported in literature led to the assignment of compound (1) as kaempferol-3-*O*-β-D-glycopyranoside (astragalin) (15).

Compound (2): all ^{1}HNMR and ^{13}CNMR signals of aglycone were confirmed by comparison with those of the previous compound (1), but in aliphatic region, the anomeric proton signal was assigned at 4.37 (d, J =1.7 Hz) and CH_3-6$^{//}$ at 0.98 (d, J = 6.8 Hz), confirmed by the anomeric carbon at 100.76 and CH_3-6$^{//}$ at 17.7. Finally, compound (2) identified as kaempferol-3-*O*-α-L-rhamnopyranoside.

Compound (3): in the aliphatic region, ^{1}HNMR Table 1 exhibited three diagnostics ^{1}H resonances at 5.31, 4.38, and 0.98 were assigned to H-1$^{//}$β (glucoside), H-1$^{///}$ α and CH3-6$^{///}$ (rhamnosyl). Terminal attachment of rhamnosyl moiety on C-6$^{//}$ of glucoside was confirmed from the characteristic downfield location of C-6$^{//}$ (68.18 ≈Δ + 7, α effect) and up field location of C-5$^{///}$ (76.33, Δ-1-1.5 ppm, β-effect). All other ^{1}H or ^{13}C resonances were assigned by comparison study with those corresponding of compounds (1), (2) and the previous reported ^{13}CNMR data of structurally related compounds. Therefore, compound (3) was finally identified as kaempferol 3-*O*-α- L- $^{1}C_4$-rhamnopyranosyl-(1$^{///}$-6$^{///}$) *O*-β-D-$^{4}C_1$-glucopyranoside (kaempferol-3-O-β-D-rutinoside).

Compound (4): in comparison with the previous compounds, broad singlet every three protons at δ 3.70 in ^{1}HNMR spectrum confirmed by the presence of carbon resonance at δ 56.09 assigned for OCH_3 group at C-4$^{/}$ were confirmed by the comparison with previously published data of structure-related kaempferide (4$^{/}$-OCH_3-kaempferol). Hence, compound (4) was identified as kaempferide-3-*O*-β-D-rutinoside.

Compound (5) was closed to compound (4), as kaempferide-3-*O*-β-D-rutinoside, in addition to the presence of other α-anomeric proton signal at 5.15 (H-1$^{////}$) and CH_3-6$^{////}$ at 0.84 (3H, d, J = 6.0 Hz) and the downfield shift (Δ+≈ 0.25) of each H-8 and H-6 at 6.70 and 6.44 respectively, were evidenced for attachment of an α-rhamnoside moiety at C-7 as *O*-glycoside, hence compound (5) was identified as the kaempferide-3-*O*-β-D rutinosid-7-*O*-α-L- rhamnopyranoside.

Compound (6): typical kaempferol-3-*O*-β-D-rutinopyranoside. In addition to the presence of α-anomeric proton signal at 5.05 assigned for extra glycone part and the downfield shift (Δ+≈ 0.25) of each H-8 and H-6 at 6.70 and 6.42 respectively were evidenced that the α-sugar moiety at C-7 as *O*-glycoside. And from the carbon resonances in ^{13}CNMR Table 1 identified the extra sugar as arabinose, hence compound (6) was confirmed as kaempferol-3-O-β-D-rutinopyranoside-7-*O*-α-D-arabinopyranoside. Phytochemical constituents were presented in Table 2 and the structure of six kaempferol derivatives isolated from *C. odorata* L. were represented in Fig. 1.

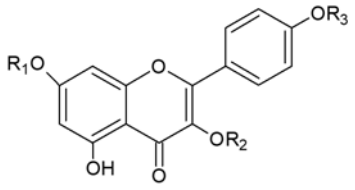

Fig. 1. Structure of six-kaempferol derivatives isolated from *Cedrela odorata* L.

Table 1. Proton and carbon-13 nuclear magnetic resonance (400 and 100 MHz, respectively) of phytoconstituents isolated from *Cedrela odorata* L.

C. No	1		2		3		4		5		6	
	^{1}H	^{13}C	^{1}H	^{13}C	^{1}H	^{13}C	^{1}H	^{13}C	^{1}H	^{13}C	^{1}H	^{13}C
2	-	156.5	-	156.5	-	Unresolved	-	156.9	-	156.8	-	156.5
3	-	133.2	-	133.2	-	133.2	-	133.3	-	133.5	-	133.2
4	-	177.3	-	177.4	-	178. 7	-	177.4	-	177.7	-	177.3
5	-	159.8	-	159.9	-	159.9	-	161.2	-	161.4	-	159.9
6	6.42 (d, *J* = 1.7 Hz)	98.7	6.42 (d, *J*=1.7Hz)	98.7	6.41 (d, *J*=1.5 Hz)	98.7	6.40	98.8	6.72 (d, J=1.8 Hz)	99.0	6.66 (d, *J*=1.2 Hz)	98.7
7		164.1		164.1		163.0		164.2		164.4		164.2
8	6.21 (d, *J* = 2.5 Hz)	93.7	6.22 (d, *J*=2.5Hz)	93.8	6.20	93.7	6.19	93.8	6.44 (d, *J*=2.1Hz)	94.1	6.45 (d, *J*=1.5 Hz)	95.0
9	-	156.8	-	156.8	-	Unresolved	-	156.5	-	157.2	-	156. 8
10	-	103.9	-	103.9	-	Unresolved	-	104.0	-	104.2	-	103.9
1'	-	120.8	-	120.9	-	120.6	-	120.9	-	121.1	-	120.9
2'	7.99 (d, *J* = 8.5 Hz)	130.8	7.98 (d, *J*=8.5Hz)	130.9	7.98 (d, *J*=8.7 Hz)	130.8	7.97 (d, *J* = 8.7 Hz)	130.9	7.97 (d, *J*=9 Hz)	131.2	7.98 (d, *J*=8.7 Hz)	130.8
3'	6.88 (d, *J* = 8.5 Hz)	115.1	6.87 (d, *J*=8.5Hz)	115.1	6.88 (d, *J* =8.7 Hz)	115.1	7 (d, *J* = 8.7 Hz)	115.1	6.87 (d, *J*=9 Hz)	115.4	6.88 (d, *J*=8.4 Hz)	115.1
4'	-	161.2	-	161.2	-	Unresolved	-	159.9	-	160.1	-	161.2
5'	6.88 (d, *J* = 8.5 Hz)	115.1	6.87 (d, *J*=8.5Hz)	115.1	6.88 (d, *J* = 8.7Hz)	115.1	7 (d, *J*=8.7Hz)	115.1	6.87 (d, J=9 Hz)	115.4	6.88 (d, *J*=8.4 Hz)	115.1
6'	7.99 (d, *J* = 8.5 Hz)	130.9	7.98 (d, *J*=8.5Hz)	130.9	7.98 (d, *J*= 8.7 Hz)	130.8	7.97 (d, *J* = 8.7 Hz)	130.9	7.97 (d, *J*= 9 Hz)	131.2	7.98 (d, *J*=8.7 Hz)	130.8
1''	5.31 (d, *J* = 7.6 Hz)	101.3	4.55 brs	100.8	5.31 (d, *J*=7.2Hz)	100.7	5.31 (d, *J*= 6Hz)	100.8	5.29 (d, *J*=7.5Hz)	100.9	5.31 (d, *J*=6.9 Hz)	101.3
2''	-	74.2	-	70.3	-	74.1	-	74.2	-	74.4	-	74.1
3''	-	76.3	-	70.6	-	76.3	-	76.4	-	76.6	-	76.3
4''	-	70.6	-	69.9	-	70.3	-	70.4	-	70.2	-	70.3
5''	-	75.7	-	71.8	-	75.7	-	75.8	-	75.9	-	75.7
6''	-	61.3	0.98 (d, *J*=6.4Hz)	17.7	-	68.2	-	68.3	-	68.5	-	68.2
1'''	-	-	-	-	4.38 brs	101.2	4.37 brs	101.3	4.37 brs	101.6	4.378 brs	100.7
2'''	-	-	-	-		71.9		71.8		72.1		71.8
3'''	-	-	-	-		70.6		70.6		70.8		70.6
4'''	-	-	-	-		71.8		71.8		72.0		71.8
5'''	-	-	-	-		70.3		70.4		70.2		70.3
6'''		-	-	-	0.98 (d, *J*=6 Hz)	17.7	0.96 (d, *J*=6 Hz)	17.8	0.96 (d, *J*=6Hz)	17.9	0.98 (d, *J*=6 Hz)	17. 7
1''''	-	-	-	-	-	-		-	5.14brs	101.0	unresolvd	107.7
2''''	-	-	-	-	-	-	-	-	-	70.4		70.6
3''''	-	-	-	-	-	-	-	-	-	70.8	--	69.9
4''''	-	-	-	-	-	-	-	-	-	70.2	-	71.8
5''''	-	-	-	-	-	-	-	-	-	72.1	-	66.9
6''''	-	-	-	-	-	-	-	-	1.05 (d, *J*=6 Hz)	18.7	-	-
4'-OCH3	-	-	-	-	-		3.75	56.1	3.36	56.4	-	-

Table 2. Phytoconstituents isolated from *Cedrela odorata* L

Compounds	Nomenclature	R_1	R_2	R_3
1	Kaempferol-3-***O***-β-**D**-glucopyranoside	H	Glucose	H
2	Kaempferol-3-***O***-α-**L**-rhamnopyranoside	H	Rhamnose	H
3	Kaempferol-3-***O***-β-**D**-rutinoside	H	Rutinose	H
4	Kaempferide-3-***O***-β-**D**-rutinoside	H	Rutinose	CH_3
5	Kaempferide-3-***O***-β-**D**-rutinosyl-7-*O*-α-**L**-rhamnopyranoside	Rhamnose	Rutinose	CH_3
6	Kaempferol-3-***O***-β-**D**-rutinosyl-7-O-α-**D**-arabinopyranoside	Arabinose	Rutinose	H

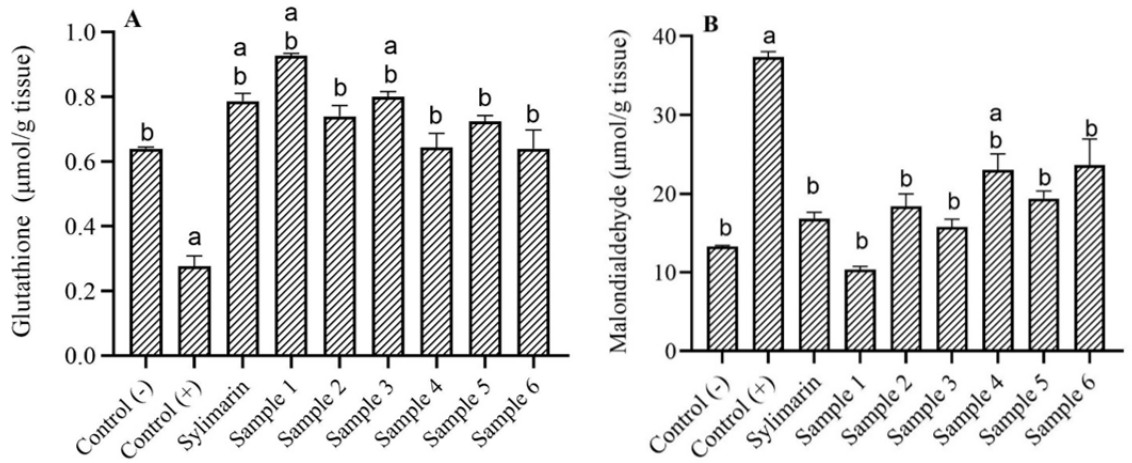

Fig. 2. (A) Effect of six glycosides from the leaves of *Cedrela odorata* L. on (A) reduced glutathione and (B) malondialdehyde in paracetamol-induced liver apoptosis. Paracetamol (positive control, 300 mg/kg), silymarin (50 mg/kg), samples 1-6 (6 isolated compounds from *Cedrela odorata* L. leaves, 100 mg/kg). Results represent mean ± SEM, n = 6. $^{a}P < 0.05$ Indicates significant differences compared with the negative control; $^{b}P < 0.05$ significantly different from the positive control.

Hepatoprotective activity

Liver oxidative stress assessment

Intraperitoneal injection of a single dose of paracetamol 300 mg/kg BW to mice significantly ($P < 0.05$) decreased the concentration of GSH, and on the other hand it significantly ($P < 0.05$) induced elevated MDA level compared to the negative control group. IP injection of silymarin and all flavonoids at 1 h prior to paracetamol injection significantly ($P < 0.05$) increased the level of GSH and on the other hand they significantly ($P < 0.05$) decreased MDA compared to the control positive control group. It was also prominent after comparison with the effect of the standard drug (silymarin) on paracetamol toxicity that the flavonoid (1) kaempferol-3-O-β-D-glycopyranoside has a significant ($P < 0.05$) ameliorative effect on GSH than that of silymarin (Fig. 2A and B).

Nitrotyrosine determination

Nitrotyrosine is a product of tyrosine nitration mediated by peroxynitrite anion and nitrogen dioxide. It is identified as a marker of cell damage. IP injection of a single dose of paracetamol at 300 mg/kg BW to mice significantly increase ($P < 0.05$) the concentration of 3-nitrotyrosine compared to negative control group. IP injection of silymarin and samples (1) kaempferol-3-O-β-D-glycopyranoside, (2) kaempferol-3-O-β-D rutinoside, (3) kaempferide-3-O-β-D-rutinoside, and (5) kaempferide-3-O-β-D rutinosyl-7-O-β-D-rhamnopyranoside 1 h prior to paracetamol injection significantly ($P < 0.05$) decreases the level of 3-nitrotyrosine compared with control positive group. Sample (4) kaempferide-3-O-β-D-rutinoside and (6) kaempferol-3-O-β-D-rutinosyl-7-O-α-D-arabinopyranoside showed no effect on paracetamol induced nitrotyrosine concentration. It was also prominent that the flavonoid (1) has a significant ($P < 0.05$) ameliorating effect as compared to silymarin (Fig. 3).

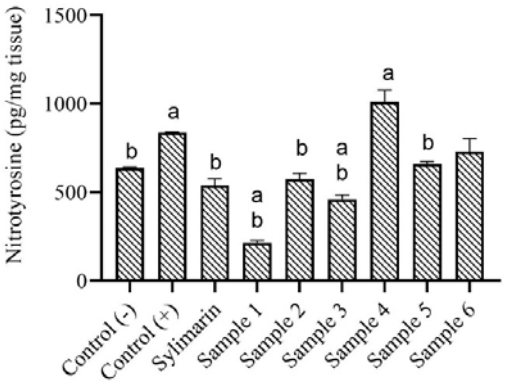

Fig. 3. Effect of six glycosides from the leaves of *Cedrela odorata L.* on 3-nitrotyrosamine in paracetamol-induced liver apoptosis. Paracetamol (positive control, 300 mg/kg), silymarin (50 mg/kg), samples 1-6 (6 isolated compounds from *Cedrela odorata* L. leaves, 100 mg/kg). Results represent mean ± SEM, n = 6. $^{a}P < 0.05$ Indicates significant differences compared with the negative control; $^{b}P < 0.05$ significantly different from the positive control.

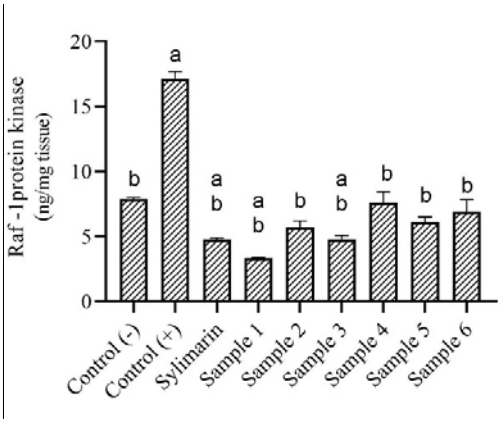

Fig. 4. Effect of six glycosides from the leaves of *Cedrela odorata L.* on Raf-1protein kinase in paracetamol-induced liver apoptosis. Paracetamol (positive control, 300 mg/kg), silymarin (50 mg/kg), samples 1-6 (6 isolated compounds from *Cedrela odorata* L. leaves, 100 mg/kg). Results represent mean ± SEM, n = 6. $^{a}P < 0.05$ Indicates significant differences compared with the negative control; $^{b}P < 0.05$ significantly different from the positive control.

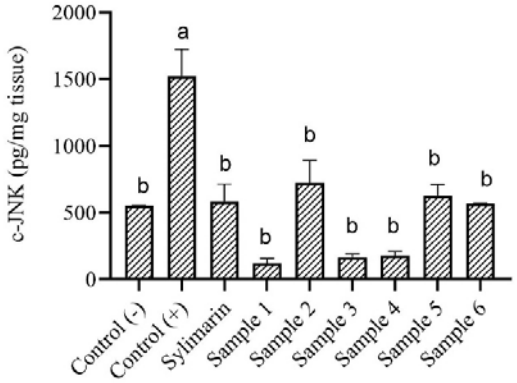

Fig. 5. Effect of six glycosides from the leaves of *Cedrela odorata L.* on c-JNK in liver apoptosis induced by paracetamol. Paracetamol (positive control, 300 mg/kg), silymarin (50 mg/kg), samples 1-6 (6 isolated compounds from *Cedrela odorata* L. leaves, 100 mg/kg). Results represent mean ± SEM, n = 6. $^{a}P < 0.05$ Indicates significant differences compared with the negative control; $^{b}P < 0.05$ significantly different from the positive control. c-JNK, C-Jun N-terminal protein kinase ½.

Apoptotic biomarkers assessment

Raf-1 protein kinase

Apoptosis triggered as a consequence of the oxidative stress was determined by increased concentrations of protein kinase Raf-1 protein in liver tissues. Our study showed that IP injection of a single dose of paracetamol 300 mg/kg significantly ($P < 0.05$) increased Raf-1 kinase as compared to the negative control group. IP injection of silymarin, as well as all flavonoid, extracts 1 h prior to paracetamol showed a significant ($P < 0.05$) decrease in Raf-1 kinase compared to the control positive group. It has been also noticed that sample (1) kaempferol-3-O-β-D-glycopyranoside has significantly ($P < 0.05$) decreased Raf-1 kinase level better than that of silymarin (Fig. 4).

C-Jun N-terminal protein kinase ½

The oxidative stress activates c-JNK which belongs to MAPK family. IP injection of a single dose of paracetamol at 300 mg/kg BW significantly ($P < 0.05$) increased c-JNK

compared to the negative control group. IP injection of silymarin and all samples (1-6) 1 h prior to IP injection of paracetamol showed a significant ($P < 0.05$) decrease in the level of c-JNK as compared to the control positive group. It was also noticed that flavonoids (1) kaempferol-3-O-β-D-glycopyranoside, (3) kaempferide-3-O-β-D-rutinoside and (4) kaempferide-3-O-β-D-rutinoside reduced the c-JNK concentration significantly ($P < 0.05$) as compared to silymarin (Fig. 5).

DISCUSSION

Oxidative stress has a crucial role in the development of paracetamol toxicity (16). The hepatotoxicity of paracetamol is characterized by the production of its metabolite; NAPQI that can be successfully scavenged by reduced glutathione (17). The paracetamol reactive metabolite; NAPQI, accumulates and results in GSH consumption, thus decreasing GSH stores. The excess NAPQI unbound to GSH may enter a rapid reaction with the mercapto groups of cellular proteins leading to the production of excessive ROS. Lipid peroxidation is initiated and in turn eventually results in hepatic architecture destruction, apoptosis, or necrosis (18). In the current study; besides their GSH enhancing effect, the administration of flavonoids (1-6) decreased the level of MDA that was triggered as a result of injection of a high dose of paracetamol. It was prominent that flavonoid (1) has a better ameliorating effect than that exerted by silymarin. The antioxidant potential of flavonoids is well-established and similar to our results; different natural phytochemicals could protect against paracetamol-induced hepatotoxicity *via* their antioxidant effect (19-21). Additionally, the hydroethanolic extract of *C. odorata L.* displayed an antihyperglycemic effect *via* its antioxidant properties and this was ascribed to the presence of active principles possessing different modes of actions. However, kaempferol glycosides were not identified nor isolated in this study (11,22).

The administration of flavonoids (1-3, and 5) and silymarin in the current study significantly decreased the level of nitrotyrosine while the flavonoids (4) and (6) showed no effect on nitrotyrosine induced by paracetamol. Also, we observed that flavonoid (1) has a better ameliorative effect than that of silymarin. The human hepatocytes respond to high doses of paracetamol by the depletion of reduced GSH and the formation of protein adducts (i.e., nitotyrosine adducts). Active NO metabolites can react with superoxide to form peroxynitrite (ONOO-) which is a powerful oxidant and nitrating agent. Subsequently, peroxynitrite reacts with tyrosine results in nitrotyrosine adducts formation. As a stable end product of peroxynitrite-mediated oxidation/nitration, nitrotyrosine can be used as NO-dependent liver damage. This oxidative stress leads to the fragility of mitochondrial membrane leading to the efflux of the cell contents and cell apoptosis (3). Similar results were obtained previously for the *Cistus laurifolius* flavonoids and the artichoke which is known to be rich in flavonoids (23-24).

Apoptosis is a form of programmed cell death that occurs in multicellular organisms (25). Apoptosis induced by paracetamol has been ruled out by studies were done by Gujral *et al*. (26). One of the most common cell death pathways involved in apoptosis is the Raf/MAP kinase pathway. This pathway, a significant signal transduction pathway in cell biology, is involved in cell cycle regulation, wound healing and tissue repair, integrin signaling, and cell migration (27). Activation of the MAPK pathway could be achieved by inducing a regulatable form of the Raf-1 kinase (28). C-Jun N-terminal kinase is activated by sequential protein phosphorylation through a MAPK module, namely, MAPK kinase (29).

In the current study, abnormal activation of Raf/MAPK signaling pathway in response to paracetamol toxicity contributed to uncontrollable cell apoptosis and was evidenced by activation of Raf-1 kinase and JNK (8). In parallel to the current findings, treatment with high doses of paracetamol leads to activation of Raf-1 proteins with the subsequent activation of JNK. This could be explained by enhanced translocation of p-JNK through the mitochondrial membrane leading to increased mitochondrial membrane permeability and membrane collapse (30-31). However, the current administration of

flavonoids (1-6) 1 h prior to paracetamol, showed a significant decrease in Raf activity as compared to the positive control group. It was also noticed that flavonoid (1) significantly reduced the level of the Raf-1 enzyme better than silymarin. Administration of flavonoids (1-6) 1 h prior to paracetamol showed a significant decrease in c-JNK as compared to the positive control group. It was also noticed that flavonoids (1), (3), and (4) significantly reduced the activity of JNK enzyme better than silymarin. Our results showed that all flavonoids (1-6) isolated from *C. odorata L.* protected against damaging effects of paracetamol *via* inhibition of Raf-1/MAP kinase pathway. This modulatory effect on the Raf/MAP kinase pathway confirmed the anti-apoptotic effect of the flavonoid glycosides that are newly isolated from the leaves of *C. odorata L.* Similarly, in a recent study performed on varicocelized rats, aspragalin (compound 1) exerted an anti-apoptotic effect by reducing the apoptotic index and the endoplasmic reticulum protein levels (p-JNK) expression leading to promoting spermatogenesis in varicocele-induced rats (32)**.**

In agreement to our findings, Tsai *et al.* (33) has described the hepatoprotective effect of the flavonoid, kaempferol, against liver injury induced by the propacetamol. Kaempferol showed antioxidant, anti-inflammatory, and anti-apoptotic activities. Similar reports showed that anti-inflammatory and antioxidant activities of kaempferol were involved in its anticancer, antidiabetic, and anti-aging effects (34). Recent reports have shown that flavonoids such as quercetin and luteolin were not likely effective in the prevention of acetaminophen hepatotoxicity as they were unable to prevent the glucuronidation step of acetaminophen metabolism (35). Kaempferol glycosides were also isolated from different plants and exhibited marked pharmacological activities (36). However, to the best of our knowledge, this is the first time in the current study to isolate kaempferol glycosides from the leaves of *C. odorata L.* and report their hepatoprotective activity through modulation of Raf-1/MAP kinase apoptotic pathway (Fig. 6).

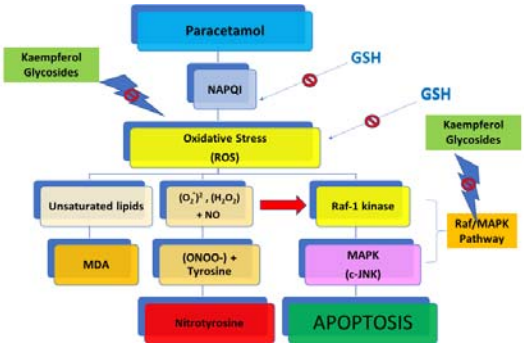

Fig. 6. Schematic diagram of the mechanisms underlying paracetamol-induced hepatotoxicity and the possible hepatoprotective effect of kaempferol glycosides on liver tissue in mice. NAPQI, N-acetyl-p-benzoquineimine; $(O_2^-)2$, superoxide; H_2O_2, hydrogen peroxide; ONOO-: peroxynitrite; MAPK, mitogen-activated protein kinase; MDA, malondialdehyde.

CONCLUSION

Our results revealed that kaempferol glycosides isolated from *C. odorata* L. leave exerted prominent antioxidant and antiapoptotic effects. It is suggested that the antiapoptotic effect might be attributed to the inhibition of Raf/MAPK pathway which is evidenced by the amelioration of Raf-1 protein kinase and c-JNK levels. According to the current findings, further molecular and clinical studies on using these kaempferol glycosides are recommended to abate paracetamol-induced hepatotoxicity.

Acknowledgments

The authors would like to thank the Pharmacology Department, National Research Centre, Egypt and Pharmacognosy Department, Faculty of Pharmacy, Al-Azhar University, Egypt for supplying instrumental facilities to conduct the current study.
Funding Information

Conflict of interest statement

Authors declared no conflict of interest in this study.

Authors' contribution

Pharmacological study had been conducted by G.F. Asaad, H.M.I. Abdallah, and Y.A. Nomier. Phytochemical studies had been conducted by H.Sh. Mohammed.

REFERENCES

1. Dkhil MA, Abdel Moneim AE, Hafez TA, Mubaraki MA, Mohamed WF, Thagfan FA, *et al*. *Myristica fragrans* kernels prevent paracetamol-induced hepatotoxicity by inducing anti-apoptotic genes and Nrf2/HO-1 pathway. Int J Mol Sci. 2019;20(4):993-1007.
   DOI: 10.3390/ijms20040993.
2. Wei G, Bergquist A, Broomé U, Lindgren S, Wallerstedt S, Almer S, *et al*. Acute liver failure in Sweden: etiology and outcome. J Intern Med. 2007;262(3):393-401.
   DOI: 10.1111/j.1365-2796.2007.01818.x.
3. Bender RP, Lindsey RH, Burden DA, Osheroff N. N-acetyl-p-benzoquinone imine, the toxic metabolite of acetaminophen, is a topoisomerase II poison. Biochemistry. 20040;43(12):3731-3739.
   DOI: 10.1021/bi036107r.
4. Placke ME, Ginsberg GL, Wyand DS, Cohen SD. Ultrastructural changes during acute acetaminophen-induced hepatotoxicity in the mouse: a time and dose study. Toxicol Pathol. 1987;15(4):431-438.
   DOI: 10.1177/019262338701500407.
5. Meyers LL, Beierschmitt WP, Khairallah EA, Cohen SD. Acetaminophen-induced inhibition of hepatic mitochondrial respiration in mice. Toxicol Appl Pharmacol. 1988;93(3):378-387.
   DOI: 10.1016/0041-008x(88)90040-3.
6. Jaeschke HA. Glutathione disulfide formation and oxidant stress during acetaminophen-induced hepatotoxicity in mice *in vivo*: the protective effect of allopurinol. J Pharmacol Exp Ther. 1990;255(3):935-941.
7. McGill MR, Jaeschke H. Metabolism and disposition of acetaminophen: recent advances in relation to hepatotoxicity and diagnosis. Pharm Res. 2013;30(9):2174-2187.
   DOI: 10.1007/s11095-013-1007-6.
8. Sweatt JD. The neuronal MAP kinase cascade: a biochemical signal integration system subserving synaptic plasticity and memory. J Neurochem. 2001;76(1):1-10.
   DOI: 10.1046/j.1471-4159.2001.00054.x.
9. Martins AP, Salgueiro LR, Da Cunha AP, Vila R, Cañigueral S, Tomi F, *et al*. Chemical composition of the bark oil of *Cedrela odorata* from *S. Tome* and *Principe*. J Essent Oil Res. 2003;15(6):422-424..
   DOI: 10.1080/10412905.2003.9698629.
10. Almonte-Flores DC, Paniagua-Castro N, Escalona-Cardoso G, Rosales-Castro M. Pharmacological and genotoxic properties of polyphenolic extracts of *Cedrela odorata* L. and *Juglans regia* L. barks in rodents. Evid Based Complement Alternat Med. 2015;2015:187346,1-9.
    DOI: 10.1155/2015/187346.
11. Giordani MA, Collicchio TC, Ascêncio SD, de Oliveira Martins DT, Balogun SO, Bieski IG, *et al*. Hydroethanolic extract of the inner stem bark of *Cedrela odorata* has low toxicity and reduces hyperglycemia induced by an overload of sucrose and glucose. J Ethnopharmacol. 2015;162:352-361.
    DOI: 10.1016/j.jep.2014.12.059.
12. Mossanen JC, Tacke F. Acetaminophen-induced acute liver injury in mice. Lab Anim. 2015;49(1_Suppl):30-36.
    DOI: 10.1177/0023677215570992.
13. Harborne TB, Mabry TJ, Mabry H. The Flavonoids. First edition. London: Springer; 1975. pp: 219.
    DOI: 10.1007/978-1-4899-2909-9.
14. Ellman GL. Tissue sulfhydryl groups. Arch Biochem Biophys. 1959;82(1):70-77.
    DOI: 10.1016/0003-9861(59)90090-6.
15. Ohakawa H, Okishi N, Yagi K. Assay for lIPid peroxides in animal tissues by thiobarbituric acid reaction. Anal Biochem. 1979;95(2):351-358.
    DOI: 10.1016/0003-2697(79)90738-3.
16. Ghobadi S, Dastan D, Soleimani M, Nili-Ahmadabadi A. Hepatoprotective potential and antioxidant activity of *Allium tripedale* in acetaminophen-induced oxidative damage. Res Pharm Sci. 2019;14(6):488-495.
    DOI: 10.4103/1735-5362.272535.
17. Mohi-Ud-Din R, Mir RH, Sawhney G, Dar MA, Bhat ZA. Possible pathways of hepatotoxicity caused by chemical agents. Curr Drug Metab. 2019;20(11):867-879.
    DOI: 10.2174/1389200220666191105121653.
18. Hamzeh M, Hosseinimehr SJ, Khalatbary AR, Mohammadi HR, Dashti A, Amiri FT. Atorvastatin mitigates cyclophosphamide-induced hepatotoxicity *via* suppression of oxidative stress and apoptosis in rat model. Res Pharm Sci. 2018;13(5):440-449.
    DOI: 10.4103/1735-5362.236837.
19. Hohmann MS, Cardoso RD, Fattori V, Arakawa NS, Tomaz JC, Lopes NP, *et al*. *Hypericum perforatum* reduces paracetamol-induced hepatotoxicity and lethality in mice by modulating inflammation and oxidative stress. Phytother Res. 2015;29(7):1097-1101.
    DOI: 10.1002/ptr.5350.
20. Rada P, Pardo V, Mobasher MA, García-Martínez I, Ruiz L, González-Rodríguez Á, *et al*. SIRT1 Controls acetaminophen hepatotoxicity by modulating inflammation and oxidative stress. Antioxid Redox Signal. 2018;28(13):1187-1208.
    DOI: 10.1089/ars.2017.7373.
21. Hu JN, Xu XY, Li W, Wang YM, Liu Y, Wang Z, *et al*. Ginsenoside Rk1 ameliorates paracetamol-induced hepatotoxicity in mice through inhibition of inflammation, oxidative stress, nitrative stress and apoptosis. J Ginseng Res. 2019;43(1):10-19.
    DOI: 10.1016/j.jgr.2017.07.003.
22. Senthilkumar R, Chandran R, Parimelazhagan T. Hepatoprotective effect of *Rhodiolaimbricata rhizome* against paracetamol-induced liver toxicity in rats. Saudi J Biol Sci. 2014;21(5):409-416.
    DOI: 10.1016/j.sjbs.2014.04.001.
23. Küpeli E, Orhan DD, Yesilada E. Effect of *Cistus laurifolius* L. leaf extracts and flavonoids on acetaminophen-induced hepatotoxicity in mice. J Ethnopharmacol. 2006;103(3):455-460.
    DOI: 10.1016/j.jep.2005.08.038.
24. El Morsy EM, Kamel R. Protective effect of artichoke leaf extract against paracetamol-induced

hepatotoxicity in rats. Pharm Biol. 2015;53(2): 167-173.
DOI: 10.3109/13880209.2014.913066.

25. Elmore S. Apoptosis: a review of programmed cell death. Toxicol Pathol. 2007;35(4):495-516.
DOI: 10.1080/01926230701320337.
25. Gujral JS, Knight TR, Farhood A, Bajt ML, Jaeschke H. Mode of cell death after acetaminophen overdose in mice: apoptosis or oncotic necrosis? Toxicol Sci. 2002;67(2):322-328.
DOI: 10.1093/toxsci/67.2.322.
26. Stacey DW. Cyclin D1 serves as a cell cycle regulatory switch in actively proliferating cells. Curr Opin Cell Biol. 2003;15(2):158-163.
DOI: 10.1016/S0955-0674(03)00008-5.
27. Shi C, Hao B, Yang Y, Muhammad I, Zhang Y, Chang Y, *et al*. JNK signaling pathway mediates acetaminophen-induced hepatotoxicity accompanied by changes of glutathione S-transferase A1 content and expression. Front Pharmacol. 2019;10:1092-1104.
DOI: 10.3389/fphar.2019.01092.
28. Cargnello M, Roux PP. Activation and function of the MAPKs and their substrates, the MAPK-activated protein kinases. Microbiol Mol Biol Rev. 2011;75(1):50-83.
DOI: 10.1128/MMBR.00031-10.
29. Han D, Ybanez MD, Ahmadi S, Yeh K, Kaplowitz N. Redox regulation of tumor necrosis factor signaling. Antioxid Redox Signal. 2009;11(9):2245-2263.
DOI: 10.1089/ars.2009.2611.
30. Kon K, Kim JS, Jaeschke H, Lemasters JJ. Mitochondrial permeability transition in acetaminophen-induced necrosis and apoptosis of cultured mouse hepatocytes. Hepatology. 2004;40(5):1170-1179.
DOI: 10.1002/hep.20437.
31. Karna KK, Choi BR, You JH, Shin YS, Cui WS, Lee SW, *et al*. The ameliorative effect of monotropein, astragalin, and spiraeoside on oxidative stress, endoplasmic reticulum stress, and mitochondrial signaling pathway in varicocelized rats. BMC Complement Altern Med. 2019;19(1):333-345.
DOI: 10.1186/s12906-019-2736-9.
32. Tsai MS, Wang YH, Lai YY, Tsou HK, Liou GG, Ko JL, *et al*. Kaempferol protects against propacetamol-induced acute liver injury through CYP2E1 inactivation, UGT1A1 activation, and attenuation of oxidative stress, inflammation and apoptosis in mice. Toxicol Lett. 2018;290:97-109.
DOI: 10.1016/j.toxlet.2018.03.024.
33. Imran M, Rauf A, Shah ZA, Saeed F, Imran A, Arshad MU, *et al*. Chemo-preventive and therapeutic effect of the dietary flavonoid kaempferol: a comprehensive review. Phytother Res. 2019;33(2):263-275.
DOI: 10.1002/ptr.6227.
34. Cao L, Kwara A, Greenblatt DJ. Metabolic interactions between acetaminophen (paracetamol) and two flavonoids, luteolin and quercetin, through *in-vitro* inhibition studies. J Pharm Pharmacol. 2017;69(12):1762-1772.
DOI: 10.1111/jphp.12812.
35. Liu HY, Peng HY, Hsu SL, Jong TT, Chou ST. Chemical characterization and antioxidative activity of four 3-hydroxyl-3-methylglutaroyl (HMG)-substituted flavonoid glycosides from *Graptopetalum paraguayense* E. Walther. Bot Stud. 2015;56(1):8-16.
DOI: 10.1186/s40529-015-0088-4.